processes

MDPI

Article

Experimental and Numerical Study of Ignition and Flame Propagation for Methane–Air Mixtures in Small Vessels

Maria Prodan [1,*], Emilian Ghicioi [1], Robert Laszlo [1], Irina Nalboc [1], Sonia Suvar [1] and Aurelian Nicola [2]

[1] National Institute for Research and Development for Mine Safety and Protection to Explosion INSEMEX, 332047 Petrosani, Romania; emilian.ghicioi@insemex.ro (E.G.); robert.laszlo@insemex.ro (R.L.); irina.nalboc@insemex.ro (I.N.); sonia.suvar@insemex.ro (S.S.)

[2] Department of Mechanical, Industrial and Transport Engineering, Petrosani University, 332006 Petrosani, Romania; Aureliannicola@upet.ro

* Correspondence: maria.prodan@insemex.ro; Tel.: +40-729939524

Abstract: Methane is one of the most common gaseous fuels that also exist in nature as the main part of the natural gas, the flammable part of biogas or as part of the reaction products from biomass pyrolysis. In this respect, the biogas and biomass installations are always subjected to explosion hazards due to methane. Simple methods for evaluating the explosion hazards are of great importance, at least in the preliminary stage. The paper describes such a method based on an elementary analysis of the cubic law of pressure rise during the early stages of flame propagation in a symmetrical cylindrical vessel of small volume (0.17 L). The pressure–time curves for lean, stoichiometric and rich methane–air mixtures were recorded and analyzed. From the early stages of pressure–time history, when the pressure increase is equal to or less than the initial pressure, normal burning velocities were evaluated and discussed. Qualitative experiments were performed in the presence of a radioactive source of ^{60}Co in order to highlight its influence over the explosivity parameters, such as minimum ignition energy, maximum rate of pressure rise, maximum explosion pressure and normal burning velocity. The results are in agreement with the literature data.

Keywords: minimum ignition energy; normal burning velocity; maximum explosion pressure; maximum rate of pressure rise; methane–air mixture

Citation: Prodan, M.; Ghicioi, E.; Laszlo, R.; Nalboc, I.; Suvar, S.; Nicola, A. Experimental and Numerical Study of Ignition and Flame Propagation for Methane–Air Mixtures in Small Vessels. *Processes* **2021**, *9*, 998. https://doi.org/10.3390/pr9060998

Academic Editor: Adam Smoliński

Received: 28 April 2021
Accepted: 1 June 2021
Published: 4 June 2021

1. Introduction

The explosion ignition and propagation in a closed space where a flammable mixture can be formed raises important safety issues for the fuel processing, storage or transport activities. After ignition, the flame spreads throughout the confined space causing a rapid release of energy, accompanied by increased pressure and emissions of heat and light. The evolution of pressure during confined explosions is the most important information needed for risk assessment and for the design of pressure vessels and pressure relief systems [1]. The explosion properties (indices) are the maximum explosion pressure, the maximum pressure rise rate, the time required to reach the maximum explosion pressure, the minimum ignition energy and the burning velocity.

Methane is one of the most studied fuels due to its occurrence as the main component of natural gas, the flammable part of biogas or as part of the reaction products from biomass pyrolysis and methanogen bacteria. Measurements of its flammability properties are periodically reported, following the update of experimental methods.

The study of methane–air explosions in closed vessels has been made in a wide range of conditions: mixtures with methane concentration between 5–15 vol.%, at various initial temperatures and pressures. In most of these studies, vessels with a low aspect ratio (length/diameter) have been used: spheres with volumes between 0.1 L and 25 m^3 [2–20]. Usually, a central position of the ignition source was chosen since this condition determines the highest explosion pressure and the highest rate of pressure rise. Some studies reported

data on explosions in elongated vessels, usually with side ignition [4]. In large vessels, buoyancy plays an important role, resulting in asymmetrical flame propagation and larger heat losses to the walls. As a consequence, the peak explosion pressures were lower in large vessels as compared to the standard vessels (V = 20 L) [3]. The discussion of pressure influence on peak explosion pressure and maximum rate of pressure rise of methane–air explosions was based on pressure measurements during closed vessel experiments at initial pressures up to 1 MPa [1]. Under extreme conditions of reactant concentrations: high concentrations of methane and oxygen and low concentrations of diluents (i.e., absence of CO_2) appear oscillating behaviors can be attributed to the occurrence of cycles of condensation and vaporization (at the vessel walls) of the water produced during the flame propagation. Such cycles culminate in the rapid phase transition of the condensed water, leading to over-adiabatic pressure peaks. The wall temperature has a significant role in preventing the occurrence of the combustion-induced rapid phase transition (CRPT). The lower limiting values of CH_4 concentration for the occurrence of the combustion-induced Rapid Phase Transition (cRPT) phenomenon have been found for $CH_4/O_2/CO_2$ and $_{CH4}/O_2/N_2$ mixtures. A region included between the lower flammability limit and the cRPT limit (LcRPT) is detected. In this region, severe pressure peaks are found. A correlation for the evaluation of these limits is also given, being extremely important for reconsidering the fuel hazards in the real process [21,22].

The minimum ignition energy is the minimum energy threshold required to initiate an explosion. Gases generally have the lowest ignition energy around the stoichiometric concentration. For this reason, the reported energies for most gases are those determined at the stoichiometric concentration. For the simulation in the laboratory of electrostatic discharges, as a frequent source of initiation of explosions of gaseous mixtures, the initiation with capacitive electrical sparks is used. Experiments over time to determine the minimum ignition energy of gaseous mixtures have shown that this parameter is influenced by several factors, including the composition of the mixture, the nature of the fuel, the initial pressure and temperature and even the presence of gamma radiation [2]. Hence, in this study, the explosion and combustion parameters, i.e., minimum ignition energy, maximum explosion pressure, maximum rate of pressure rise and laminar burning velocity, were explored and analyzed for mixtures of methane and air in the presence of a gamma radiation source. The data obtained can give additions to the database and contribute to a comprehensive view of explosion behaviors of methane. A series of experiments were performed in the presence of a closed source with the radioisotope ^{60}Co (gamma radiation source) embedded in a protective metal capsule, which ensures the ionization of the space between the electrodes through the transparent window of the explosion cell. As it was not possible to measure the intensity of the radiation in the space between the electrodes, the results are qualitative, allowing, however, to highlight its influence on the explored parameters.

There is a good positive correlation between the high-temperature environment formed by coal spontaneous combustion in goaf and the radon exhalation in coal. The higher the temperature is, the greater the radon exhalation will be. Increasing concentrations of released radon gas will accumulate in an enclosed goaf and ultimately migrate upwards to form a radon anomaly on the ground surface. Based on this principle, the surface-based radon detection method can determine the location of underground hidden heat sources by detecting high-concentration radon areas on the ground [23]. Given the known explosion hazards found in this kind of workplace and the possibility of the radioactive source to be present, it is considered that more extensive studies to be performed in order to evaluate the influence over the explosivity parameters.

The pressure–time history during deflagration of premixed fuel–air flammable mixtures in a closed vessel has been widely used to determine the laminar burning velocities [24]. The procedures and limitations regarding the use of the whole pressure–time curves have been critically analyzed and discussed [25,26]. In the recent studies that used propagating spherical laminar flames monitored by optical methods only a short time after ignition, when the disturbances caused by the energy input at ignition, the flame

curvature, and the varying flame thicknesses are small, were reported improved values for CH_4–air mixtures burning velocities, corrected for flame stretch [27–30]. Other models used only p(t) measurements over longer periods, i.e., from ignition up to the inflection point p(t) records. The laminar burning velocities of CH_4–air mixtures were determined using models for either thin flames [24,31] or thick flames [24,32]. Stationary flames anchored on burners were also used to determine the laminar burning velocity of methane with air or air + inert additives using the heat flux method [33]. Stagnation flames allowed the determination of stretch-free laminar flame speeds of CH_4–air mixtures over extensive ranges of stoichiometry, pressure, and flame temperature [34]. Another recent method used data obtained in a preheated high-aspect-ratio diverging channel [35]. Duva et. al [29] measured the flame front radius (Rf), schlieren photography was employed for methane–air SEF at constant pressure in the Michigan State University constant volume combustion chamber, using CHEMKIN-PRO, the expansion ratio was numerically determined with the GRI-Mech 3.0 mechanism. The Rf data was obtained with a z-type Schlieren, and they found for the stoichiometric concentration a S_u 47 cm/s for methane air mixtures. Correlations for the laminar burning velocity and burned gas Markstein length of methane–air mixtures diluted with flue gases at high temperatures and pressures. Various advantages and disadvantages are inherently associated with each of the techniques for measuring the laminar burning velocity. For instance, the spherical flame method is commonly used for measuring the laminar burning velocity at high pressures. The approach is susceptible to flame instabilities for combustible mixture with non-unity Lewis number (Le = a/D, where a is the thermal diffusivity and D is mass diffusivity). A change in the area of the propagating flame front with time due to aerodynamic and boundary conditions is called the flame stretch, and it is defined as the logarithmic rate of change of flame area with time. Corrections due to flame stretch are required for obtaining the accurate magnitude of the laminar burning velocity [36].

A different approach has been recently proposed [37] based on the use of early stages of pressure–time evolution assumed to follow the cubic law, $\Delta P \sim t3$. The approach was successfully applied to several flammable systems [38–43]. In the present paper, the normal burning velocities of lean, stoichiometric and rich CH_4–air mixtures were measured using the early stages of pressure evolution in a closed vessel, following the spark ignition.

In the present paper, data on the constant volume combustion of methane–air mixtures in various initial conditions (pressures within 100–150 kPa and methane concentrations within 7–12 vol.%) at ambient initial temperature are reported. Experiments were performed in a cylindrical closed with central ignition.

2. Materials and Methods

The gaseous mixture containing 7%, 8%, 9%, 9.5%, 10% and 12% methane in the air were successively prepared in stainless steel cylinders at 4 bar total pressure by partial pressure method using methane 99.99% purity from SIAD and used 24 h after mixing. Methane–air mixtures were studied, in the concentration range (between 7% and 12% vol.), at variable initial pressure (between 0.8 and 1.50 bar) using the constant volume bomb method.

The experiments were carried out in a cylindrical explosion vessel with diameter equal to height: Φ = h = 6 cm (V_0 = 0.17 L) and with a radius of the equivalent spherical volume R* = 3.434 cm) given in Figure 1. The explosion pressure was monitored with a Kistler 601A piezoelectric transducer coupled to a type 5011B load amplifier. The technical data of the pressure transducer are the following: range 0–250 bar, sensitivity —16 pC/bar, linearity ±0.5%, uncertainty at an expansion coefficient k = 20.3 bar.

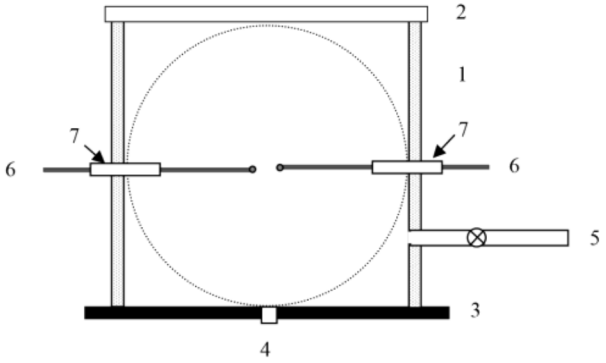

Figure 1. Explosion vessel: 1—vessel body; 2—transparent top cover; 3—bottom cover; 4—pressure transducer; 5—feeding/evacuation pipe with tap; 6—high voltage electrodes; 7—electric insulation.

A typical diagram p (t) recorded during the explosion of a 9% methane–air mixture at the initial temperature of T_0 = 298 K and initial pressure P_0 = 1 bar (100 kPa) is shown in Figure 2 together with its derivative. The derivation of the p (t) curve was performed after a prior smoothing using the Savitzky–Golay method. This involves the analysis of 500–700 points in the range $0 \leq t \leq \theta_{max}$. In all cases, a smoothing level of 5% was used, as a smoothing performed at a higher level (for example, 20%) leads to both noise reduction and signal distortion.

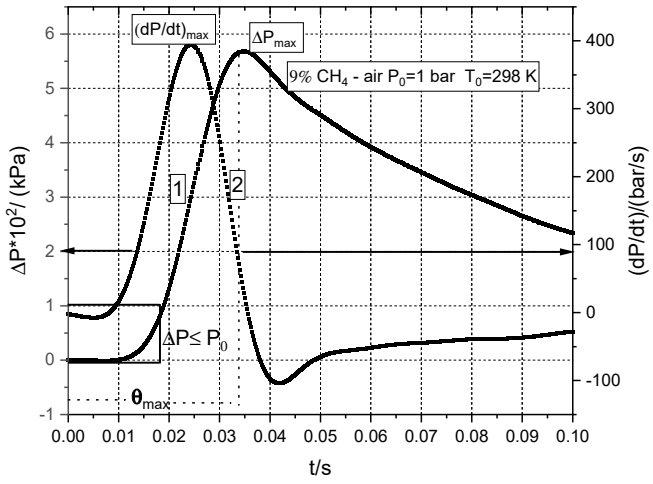

Figure 2. An illustration of the experimental pressure–time curve, ΔP–t, its calculated derivative (dP/dt)–t and resulted characteristic parameters ΔP_{max} (curve 1) and $(dP/dt)_{max}$ (curve 2), θ_{max}. The initial pressure rise for $\Delta P \leq P_0$ is shown on the lower left side.

For the generation of high voltage capacitive discharges, a new system was built, different from those reported in the literature and feasible with components purchased from well–known companies or with some artisanal components. The circuit shown in the block diagram in Figure 3 generates a voltage ramp in order to slowly charge the high voltage capacitor C. The voltage on the capacitor increases until the breakthrough voltage is reached between the electrodes of the CELL (explosion vessel).

Thus, an electric discharge occurs in the explosion cell, which, if it has sufficient energy, can ignite the introduced gas mixture. The energy transmitted to the cell by capacitor C is given by the relation below:

$$W = \frac{C \times \left(V_{02i} - V_{02f}\right)^2}{2} \quad (1)$$

where W is the energy supplied to the spark; C is the capacity of the high voltage capacitor; V_{02i} is the initial voltage at the capacitor terminals at the beginning of the discharge; V_{02f} is the final voltage on the capacitor after the spark is extinguished.

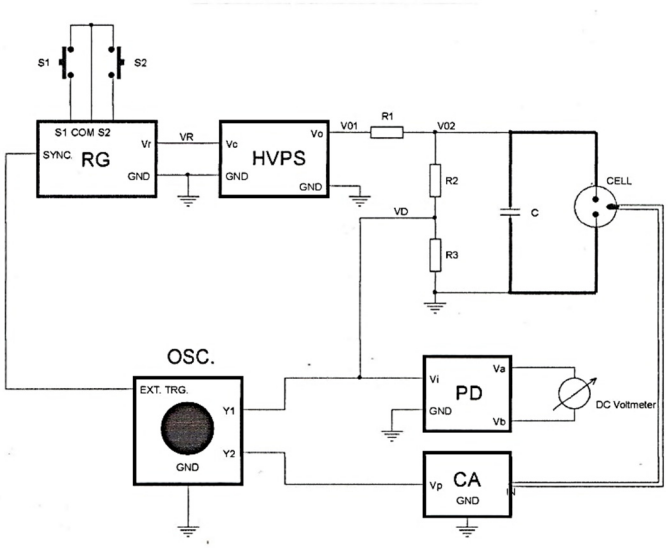

Legend:
RG—Voltage ramp generator
S1, S2—START and STOP buttons, respectively
HVPS—Controlled high voltage source
CELL—Explosion vessel
C—High voltage capacitor
R1, R2, R3—High voltage resistors
PD—Peak detector
DC Voltmeter—DC voltmeter
CA—Load amplifier
OSC—2-channel oscilloscope

Figure 3. A block diagram for the generation of the capacitive sparks.

The maximum rates of pressure rise $(dp/dt)max$ were computed from pressure–time diagrams after smoothing the p(t)data by Savitzky–Golay method, based on the least–squares quartic polynomial fitting across a moving window within the data. The method, described in [1,40] in previous papers, has the advantage of producing a smoothed first derivative without filtering the data. In all cases, we used a 5% smoothing level.

3. Results and Discussion

The key to preventing uncontrolled explosions is the determination of the flammability properties in various conditions. The main parameters that are usually used in explosion protection are the flammability limits, minimum ignition energy, maximum rate of pressure rise, maximum explosion pressure, explosion index and normal burning velocity. Based on the experimental determinations and numerical calculations, all the equipment and processes are specially dimensioned in order to satisfy the safety measures.

3.1. Influence of Initial Pressure and Initial Composition on Normal Burning Velocity

Normal burning velocity is a basic property of a combustible mixture, influenced by the overall combustion rate in the flame front and is dependent on the various parameters such as fuel type, initial temperature and pressure, fuel–to–oxygen ratio and the inert gases presence in the mixture [43]. The normal burning velocity is used for the design of venting devices in processes that are susceptible to forming explosion atmospheres or for the modeling of turbulent flame propagation in computational fluid dynamics. There are several methods for the determination of the normal burning velocity, for example, by using stationary flames such as the burner method or the counter–flow twin flames method or non–stationary flames (the tube method or the constant volume method). The constant volume method, where the normal burning velocity is evaluated from pressure–time records obtained during centrally ignited explosions in various initial conditions, is frequently used [44–46].

The normal burning velocity was calculated from the cubic law coefficient of pressure rise in the early stage of flame propagation in a closed vessel, k, by assuming isothermal compression of unburned gas ahead the flame front [37]:

$$S_u = R_c \times \left(\frac{k_3}{\Delta P_{max}}\right)^{1/3} \times \left(\frac{P_0}{P_{max}}\right)^{2/3}, \quad (2)$$

where R_c is the radius of the sphere with a volume equivalent to the volume of the cylindrical cell.

It was observed that during the initial stage of flame propagation, the pressure increase is proportional to the time at the third power:

$$\Delta P = k_3 \times t^3 \quad (3)$$

where k_3 is a factor that can be correlated with the normal burning velocity, S_u, measured with reference to the unburned gas.

Due to the random fluctuations of both the abscissa and the ordinate during the recording of the pressure over time, an improved correlation equation with three adjustable parameters proved to be more suitable for fitting on the experimental data for the early stage, $\Delta P \leq P_0$ [37]:

$$\Delta P = a_0 + k_3 \times (t - \tau)^3 \quad (4)$$

where a_0 and τ are two adjustable parameters accounting for different random deviation of the curve, and k_3 is a parameter related to the burning velocity

From Equations (2)–(4), it can be observed that the method requires only measurable properties and can be applied to mixtures of unknown nature and composition.

The normal burning velocities of methane–air at various initial pressures and ambient initial temperature are plotted against methane concentration in Figure 4 along with the best-fit correlations of data as second–order polynomials. The smoothed peak burning velocity at 1 bar is S_u = 46 cm s^{-1}, which is well within the range of values reported from the literature (41 cms^{-1}) [20]. The initial pressure increase generates a decrease in normal burning velocities for all examined mixtures.

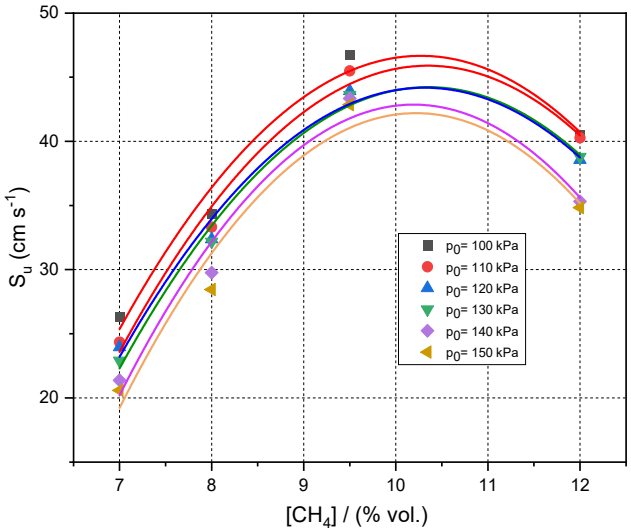

Figure 4. Normal burning velocities of CH_4–air at various initial pressures; experimental data.

A comparison between the normal burning velocities of methane–air at ambient initial and the normal burning velocities in the presence of a radioactive source is plotted in Figure 5. The data were fitted by second–order polynomials. The burning velocities of methane–air in the presence of the Cobalt source were up to 4% lower than in normal

conditions, taking into consideration that the experimental error was preserved in both situations, respectively, with or without radiation source. The experimental error was calculated to 2.6%, with an expansion coefficient k = 2 without considering the intensity of the radiation. More investigations are needed in the presence of measured intensity radioactive sources.

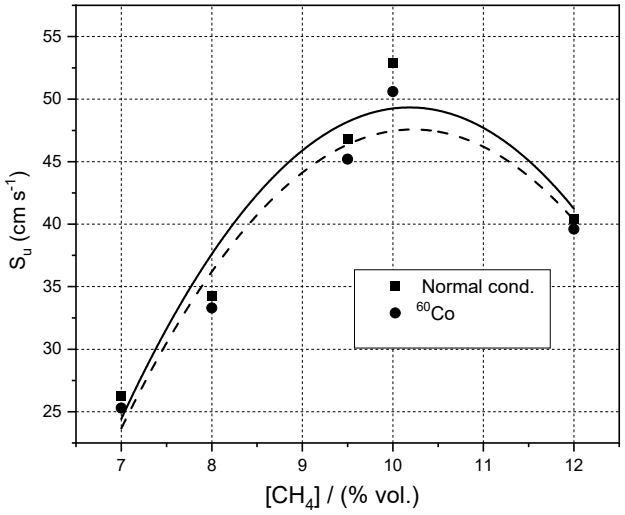

Figure 5. Normal burning velocities of CH_4–air at various initial concentrations in the presence of radiation from ^{60}Co; experimental data.

The variation of S_u with the initial pressure is usually rationalized with a power law:

$$S_u = S_{u,0} \times (P/P_{ref})^{\nu} \quad (5)$$

where P_{ref} is the reference pressure, taken usually as P_{ref} = 100 kPa, and ν is the baric coefficient of the normal burning velocity. The baric coefficients resulted from the linear regressions $\ln(S_u)$ against $\ln(P/P_{ref})$ are given in Table 1. For the stoichiometric mixtures, the obtained value ($\nu = -0.214$) is within the range of the literature data from -0.17 [47] to -0.50 [48]. Besides its value for prediction of the normal burning velocity within a certain pressure range, the baric coefficient of the normal burning velocity can also be used to evaluate the overall reaction order n_r within the flame, according to Equation (6) [48],

$$n_r = 2(1 + \nu) \quad (6)$$

and obtaining n_r = 1.57, in accord with similar data for other hydrocarbon/air mixtures [42].

Table 1. Experimental normal burning velocities, S_u, baric coefficients of normal burning velocity, ν, overall reaction orders n_r resulted from S_u, variation with methane concentration (φ is the equivalence ratio), at P_0 = 100 kPa.

% CH_4	φ	S_u/(m/s)	$-\nu$	n_r (from ν)
8.0	0.83	0.343	0.458	1.084
9.5	1.00	0.467	0.214	1.572
10	1.06	0.518	0.387	1.226
12	1.30	0.404	0.405	1.190

The results obtained in the present study shows again that by using the coefficients of the cubic law in the early stage of the explosion process, range well within the literature data, obtained experimentally for stoichiometric mixture is almost the same with the S_u value obtained by Duva et al. [29]. Besides the fact that the method does not imply physical and chemical properties of the fuel, the advantage is that the small vessel can be used

for performing a greater number of experiments in a shorter time with a smaller quantity of flammable substances; hence, the experimental hazard in performing the physical experiments is lower.

3.2. Influence of Initial Pressure, Initial Composition and Radioactive Source on Minimum Ignition Energy

The minimum ignition energies determined experimentally are given in Table 2. It is observed that the energy values are minimal around the stoichiometric concentration and increase towards the limits of the explosion range.

Table 2. Experimentally determined minimum ignition energies in the explosion cell with a volume of 0.17 L, with $\Phi/h = 1$, by varying the initial pressure and the concentration of CH_4.

[CH_4] % vol.	**P_0 = 100 kPa**	**P_0 = 150 kPa**
7	1.21	1.12
8	0.79	0.90
9	0.64	0.66
9.5	0.61	0.53
10	0.64	0.56
12	2.82	2.15

In Figure 6, the variation of the minimum ignition energy with the initial pressure and methane concentration is also observed, the highest values obtained being for the sub-atmospheric pressure, 80 kPa, and the lowest values being obtained for the initial pressure of 150 kPa. The minimum value obtained using the experimental setup described, respectively, by initiation with high voltage capacitive electrical sparks, is in good agreement with the data reported in the literature, although the minimum value is double that reported by Lewis and von Elbe [49].

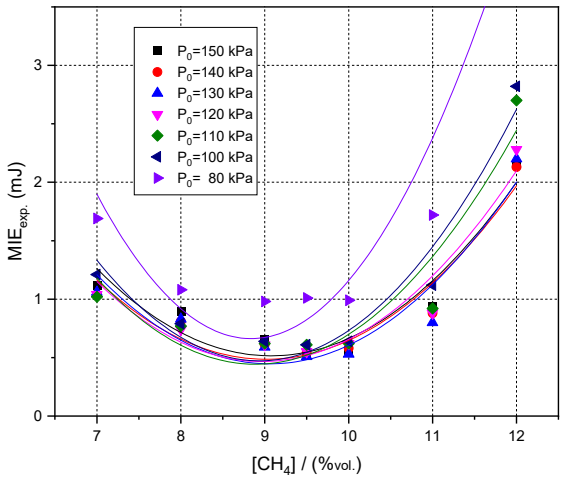

Figure 6. The variation of minimum ignition energy for CH_4–air mixtures at different initial pressures and methane concentrations.

The energies determined on the current system are calculated based on the charging voltage and capacitor capacity. This energy is actually the energy stored between the capacitor armatures so that when the capacitor is discharged through the spark, only part of this energy is given to the spark, the difference remaining in the capacitor as residual energy, given that the electric arc between the electrodes is interrupted before consuming the whole energies, more precisely when the potential difference between the electrodes

fails to achieve the ionization of the gas between the electrodes. However, the contribution of residual energy remains quite small, as it results from the relation [49]:

$$\text{MIE} = 0.5 \times \text{C} \times \text{U}^2 \quad (7)$$

where the breakthrough voltage is of the order of kilovolts and the residual voltage is a few hundred volts and C represents the capacity and U the voltage. Over time, a large number of experimental studies have been performed to determine the value of the minimum ignition energy for different combustible hydrocarbons, depending on the composition of the mixture, the method of generating the spark and the properties of the electrical circuit. It should be noted that the values of the minimum ignition energies reported by other researchers, such as Moorhouse or Eckhoff [50], were generally higher than those determined by Lewis and von Elbe [49].

Analyzing the results obtained to determine the minimum ignition energy in the presence of the radioactive source of ^{60}Co, the results presented in Table 3 and comparative for the initial ambient pressure in Figure 7, it is observed that, similar to the determinations in the absence of the radioactive source, the energy values are minimal around the stoichiometric concentration and increase towards the limits of the explosion range.

Table 3. Experimentally determined minimum ignition energies in the explosion cell with a volume of 0.17 L, with Φ/h = 1, by varying the initial pressure and the concentration of CH_4 in the presence of ^{60}Co radioactive source.

[CH_4] % vol	MIE [mJ] at P_0 = 100 kPa	MIE [mJ] at P_0 = 150 kPa
7	1.00	1.19
8	0.85	0.74
9	0.58	0.58
9.5	0.52	0.54
10	0.55	0.61
12	2.02	–

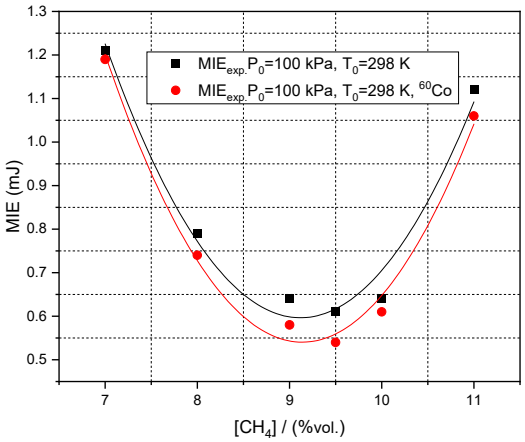

Figure 7. Variation of minimum ignition energy for CH_4–air mixtures in the presence of radioactive ^{60}Co source.

From Table 4, where the percentage decrease in MIE is represented in the presence of the ^{60}Co radioactive source, it is observed that there are differences of up to 15% between the values obtained by the two methods presented. The experimental error for the determination of minimum ignition energy was calculated to be 4.7% for an expansion coefficient k = 2, taking into consideration that the experimental error was preserved in all situations. Even though there is not a clear pattern, it is obvious that there is an influence, and these findings need to be further investigated in a separate work focused on the influence of radiation over the generating species in the first stage of ignition.

Table 4. MIE decrease in the presence of the ^{60}Co radioactive source.

[CH_4] % vol.	−ΔMIE [%] at P_0 = 80 kPa	−ΔMIE [%] at P_0 = 100 kPa	−ΔMIE [%] at P_0 = 150 kPa
7	14.8	1.65	10.7
8	1.85	6.33	5.6
9	3.06	9.38	12.1
9.5	1.98	11.5	1.89
10	11.1	4.69	1.79
12	–	5.36	6.38

The experimental method used in previous research requires that high voltage be present on the electrodes for a considerable period of time. The extended duration of action of the high voltage allows the ionization of the gas, thus reducing the dielectric constant of the gas. This leads to the reduction of the current voltage, which can affect the calculation of energy based on equation 7. Lewis and von Elbe [49] used radium capsules of various powers inside the blast cell to reduce the time between voltages charging and spark ignition, thus reducing the value of the minimum ignition energy determined.

In this paper, we tried to assign a practical application of this phenomenon, in the sense that, in these conditions, the possibility of reducing the minimum ignition energy in the presence of gamma radiation suggests reassessing the safety conditions required in workplaces where this phenomenon may occur, especially related to electrical equipment with intrinsic safety explosion proof protection used for monitoring of processes from various installation such as those used for the generation of biogas.

3.3. Influence of Initial Pressure and Initial Composition on Peak Explosion Pressures and Maximum rate of Pressure Rise in Normal and Radioactive Conditions

For each flammable composition, the peak explosion pressure was influenced by the initial pressure. Typical graphs for explosions are shown in Figure 8, where data measured at various initial pressures have been plotted. In both figures, the best-fit lines, by 2nd order polynomials, have been drawn as well.

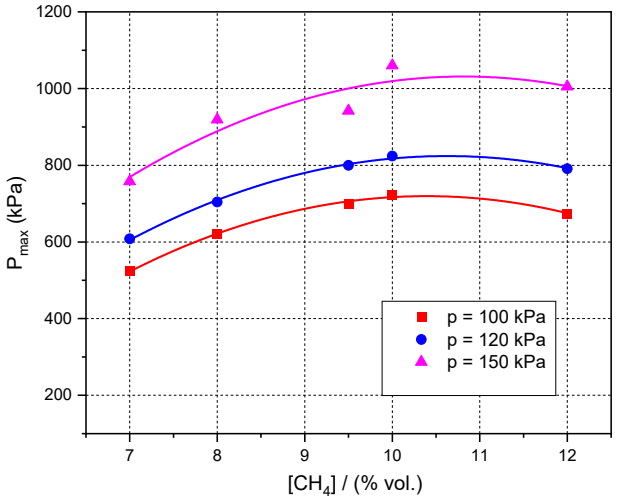

Figure 8. Experimental maximum explosion pressures at different initial pressures and composition.

A comparison of peak explosion pressures obtained in normal conditions and in the presence of radioactive sources can be seen in Figure 9, where little data from literature were also plotted. A more comprehensive comparison of our results with reference data from literature can be found in Table 5.

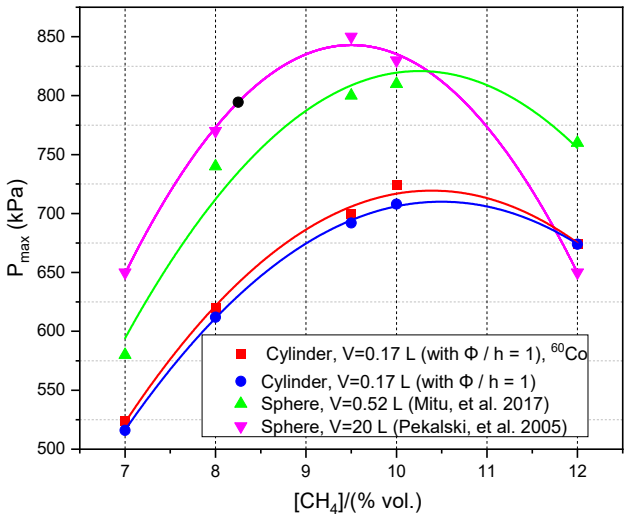

Figure 9. Experimental maximum explosion pressures for CH_4–air mixtures at ambient initial conditions and in the presence of the radioactive ^{60}Co source.

Table 5. Experimental explosion pressures of methane–air mixtures in vessels with central ignition at ambient initial conditions at 9.5% vol.

P_{max}/kPa	Reference
700	Cylinder, V = 10 m^3 [51], Cylinder V = 0.17 L, with Φ/h = 1, present data
720	Sphere, V = 20 L [9]
770	Sphere V = 20 L [12]; Cylinder, V = 22 L, L/D = 1.15 [14]); Cylinder, V = 5.34 L, L/D = 1.17 [52]
790	Sphere, V = 20 L [17–19]

The variation of maximum rates of pressure rises against methane composition at various initial pressures is shown in Figures 10 and 11, where data obtained in normal conditions and in the presence of a radioactive source were plotted. The rates of pressure rise increase with the increasing initial pressure at all methane concentrations. In both cases and at each examined pressure, the maximum rates of pressure rise reach a peak for CH_4–air mixtures at the same concentration range where highest peak pressures were measured, namely stoichiometric and as it is called the most reactive concentration, approx. 10%.

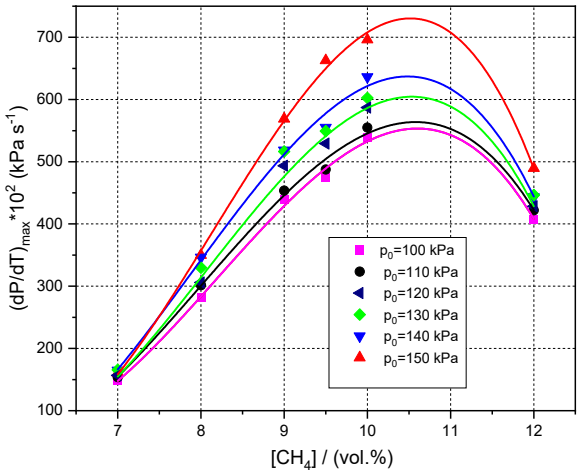

Figure 10. Experimental maximum rate of pressure rises at different initial pressures and composition for CH_4–air mixtures.

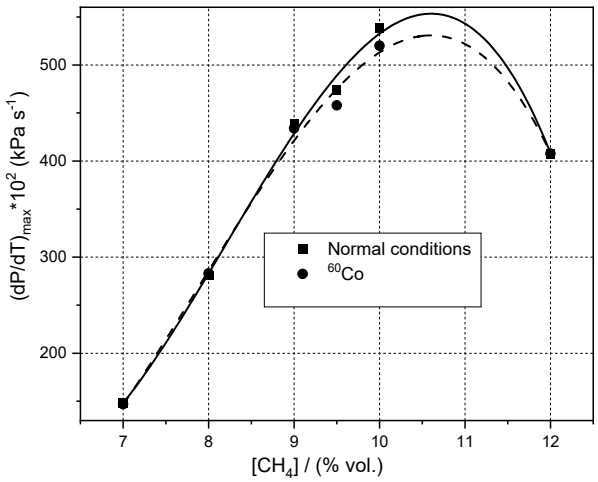

Figure 11. Experimental maximum rate of pressure rises for CH_4–air mixtures at ambient initial conditions and in the presence of ^{60}Co.

A comparison between the present results and literature data can be made by means of the severity factor *KG*, calculated as:

$$K_g = \left(\frac{dP}{dt}\right)_{max} \times \sqrt[3]{V}, \quad (8)$$

where V is the volume of the explosion vessel.

In the present paper, the measurements in the cylindrical vessel with low volume, at stoichiometric CH_4–air mixture, in our case, 26 bar·m·s^{-1} range within the literature data, for example, at measurements performed in cylindrical vessels K_G with explosion vessels volume significantly higher ranges between 11 bar·m·s^{-1} [3] and 90 bar·m·s^{-1} [5].

4. Conclusions

The importance of studying the early stage of the closed vessel combustion process lies in the practical applicability of knowing the normal burning velocity. Experimentally determined normal burning velocities are important for the design of venting systems of the pressurized vessels. The burning velocities of methane–air mixtures obtained from the records of pressure during explosions in a cylindrical vessel with central ignition, using the coefficients of the cubic law in the early stage of the process, range well with literature data obtained by other measuring techniques. It can be stated that the method is simple and reliable, and because the computing does not imply physical or chemical properties, the method can be used in complex systems.

An important advantage is the use of a small vessel for the determinations of the explosion properties, given the fact that the experimental results are well fitted with the literature data. In this respect, there can be performed a greater number of experiments in a shorter time with a smaller quantity of flammable substances.

The minimum ignition energy of methane–air mixtures was determined experimentally by means of a capacitive discharge initiation system with the generation of a high voltage electric spark. Reporting the data obtained to similar results in the literature highlighted that the minimum value obtained using the experimental setup used, taking into account the capacitive residual energy of the system, is in good agreement with the data reported in the literature.

Analyzing the existing data in the literature regarding the properties of coals, in which the presence of radioactive elements was reported, it was considered useful to reproduce in the laboratory these particular conditions. In this regard, experimental tests were performed to determine the minimum ignition energy and the propagation properties such as normal burning velocity, maximum explosion pressure and maximum rate of

pressure rise in the presence of a gamma radiation source, with the radioisotope ^{60}Co, embedded in a protective metal capsule, by positioning it on the transparent window of the explosion cell. The results allow highlighting the influence of gamma radiation on the minimum ignition energy. More extensive studies need to be performed in order to quantify the influence of specific radioactive sources over the explosion parameters.

As a result of the decrease in the minimum ignition energy for the air–methane mixture in the presence of radioactive sources, it is considered necessary to reconsider the explosion risk assessment for workplaces endangered by the presence of radiation and flammable gases.

Based on the experimental determinations and numerical calculations, all the equipment and processes are specially dimensioned in order to satisfy the safety measures. More than that, the employers are required to perform the explosion risk assessment for industrial activities in potentially explosive atmospheres, which requires knowledge of the explosion parameters presented in the paper.

The findings in the present paper suggest that considering that there is an influence of a gamma radiation source over the explosivity parameters, the safety conditions required at the workplace need reassessing, especially related to electrical equipment with intrinsic safety explosion proof protection.

As a prospective research activity: the identification of an area with industrial activity endangered by ionization radiation (within limits that are not dangerous for the human body) and flammable gases, capable of forming explosive mixtures and conducting in-depth research on changing explosion parameters and developing proposals to improve prevention and protection measures.

Author Contributions: Conceptualization, M.P.; Data curation, A.N.; Formal analysis, A.N.; Writing—original draft, M.P. and E.G.; Writing—review and editing, R.L., I.N. and S.S. All authors have read and agreed to the published version of the manuscript.

Funding: This research received no external funding.

Data Availability Statement: The data reported for the minimum ignition energy variation in the presence of a radioactive source can be found in the doctoral thesis of Maria Prodan, https://www.chimie.unibuc.ro/images/teze_de_doctorat/2017-04-28-Prodan/Rezumat_ROM.pdf (accessed on 4 May 2021).

Conflicts of Interest: The authors declare no conflict of interest.

References

1. Mitu, M.; Giurcan, V.; Razus, D.; Prodan, M.; Oancea, D. Propagation Indices of Methane-Air Explosions in Closed Vessels. *J. Loss Prev. Process. Ind.* **2017**, *47*, 110–119. [CrossRef]
2. Bartknecht, W.; Zwahlen, G. *Explosionsschutz: Grundlagen Und Anwendung*; Springer: Berlin/Heidelberg, Germany, 1993.
3. Cashdollar, K.; Zlochower, I.; Green, G.; Thomas, R.; Hertzberg, M. Flammability of Methane, Propane, and Hydrogen Gases. *J. Loss Prev. Process. Ind.* **2000**, *13*, 327–340. [CrossRef]
4. Gant, S.E.; Pursell, M.R.; Lea, C.J.; Fletcher, J.; Rattigan, W.; Thyer, A.M.; Connolly, S. Flammability of Hydrocarbon and Carbon Dioxide Mixtures. *Process. Saf. Environ. Prot.* **2011**, *89*, 472–481. [CrossRef]
5. Gieras, M.; Klemens, R.; Rarata, G.; Wolanski, P. Determination of explosion parameters of methane-air mixtures in the chamber of 40 dm^3 at normal and elevated temperature. *J. Loss Prev. Process. Ind.* **2006**, *19*, 263–270. [CrossRef]
6. Gieras, M.; Klemens, R. Experimental studies of explosions of methane-air mixtures in a constant chamber. *Combust. Sci. Technol.* **2010**, *181*, 641–653. [CrossRef]
7. Holtappels, K. *Report on the Experimentally Determined Explosion Limits, Explosion Pressures and Rates of Explosion Pressure Rise*; SAFEKINEX project Part I: Methane, hydrogen and propylene; Deliverable 8; Federal Institute for Materials Research and Testing (BAM): Berglin, Germany, 2006.
8. Holtappels, K.; Passman, H. *Interpretation of Gas. Explosion Tests; Extremes in Explosion Severity*; SAFEKINEX project; Deliverable 10; Federal Institute for Materials Research and Testing (BAM): Berglin, Germany, 2007.
9. Ma, Q.; Zhang, Q.; Chen, J.; Huang, Y.; Shi, Y. Effects of hydrogen on combustion characteristics of methane in air. *Int. J. Hydrogen Energy* **2014**, *39*, 11291–11298. [CrossRef]
10. Mashuga, C.; Crowl, D. Application of the flammability diagram for evaluation of fire and explosion hazards of flammable vapors. *Proc. Saf. Progr.* **1998**, *17*, 176–183. [CrossRef]

11. Pekalski, A.A.; Schildberg, H.P.; Smallegange, P.S.D.; Lemkowitz, S.M.; Zevenbergen, J.F.; Braithwaite, M.; Pasman, H.J. Determination of the explosion behaviour of methane and propene in air or oxygen at standard and elevated conditions. *Process. Saf. Environ. Prot.* **2005**, *83*, 421–429. [CrossRef]
12. Prodan, M.; Ghicioi, E.; Oancea, D. Correlation of explosion parameters and explosion type events for preventing environmental pollution. *Environ. Eng. Manag. J.* **2014**, *13*, 1409–1414. [CrossRef]
13. Sapko, M.J.; Furno, A.L.; Kuchta, J.M. Flame and pressure development of large-scale CH_4–air–N_2 explosions. *US Bur. Mines Rep. Investig.* **1976**, *8*, 176.
14. Senecal, J.; Beaulieu, P.K.G. New data and analysis. *Process. Saf. Progr.* **1998**, *17*, 9–15. [CrossRef]
15. Wang, Z.R.; Ni, L.; Liu, X.; Jiang, J.C.; Wang, R. Effects of N_2/CO_2 on explosion characteristics of methane and air mixture. *J. Loss Prev. Process. Ind.* **2014**, *31*, 10–15. [CrossRef]
16. Wu, S.Y.; Lin, N.K.; Shu, C.M. Effects of flammability characteristics of methane with three inert gases. *Proc. Saf. Progr.* **2010**, *29*, 349–352. [CrossRef]
17. Zhang, Q.; Li, W.; Lin, D.C.; Duan, Y.; Liang, H.M. Experimental study of gas deflagration temperature distribution and its measurement. *Exp. Therm. Fluid Sci.* **2011**, *35*, 503–508. [CrossRef]
18. Zhang, Q.; Li, W.; Zhang, S. Effects of spark duration on minimum ignition energy for methane/air mixture. *Proc. Saf. Progr.* **2011**, *30*, 154–156. [CrossRef]
19. Zhang, Q.; Li, W. Ignition characteristics for methane-air mixtures at various initial temperatures. *Process. Saf. Progr.* **2013**, *32*, 37–41. [CrossRef]
20. Zhang, B.; Xiu, G.; Bai, C. Explosion characteristics of argon/nitrogen diluted natural gas–air mixtures. *Fuel* **2014**, *124*, 125–132. [CrossRef]
21. Di Benedetto, A.; Cammarota, F.; Sarli, V.; Salzano, E.; Russo, G. Anomalous behavior during explosions of CH_4 in oxygen-enriched air. *Combust. Flame* **2011**, *158*, 2214–2219. [CrossRef]
22. Di Benedetto, A.; Cammarota, F.; Sarli, V.; Salzano, E.; Russo, G. Reconsidering the flammability diagram for $CH_4/O_2/N_2$ and CH4/O2/CO2 mixtures in light of combustion-induced Rapid Phase Transition. *Chem. Eng. Sci.* **2012**, *8*, 142–147. [CrossRef]
23. Zhou, B.; Deng, C.; Hao, J.; An, B.; Wu, R. Experimental study on the mechanism of radon exhalation during coal spontaneous combustion in goaf. *Tunn. Undergr. Space Technol.* **2021**, *113*, 103776. [CrossRef]
24. Dahoe, A.E.; de Goey, L.P.H. On the determination of the laminar burning velocity of closed vessel explosions. *J. Loss Prevent. Proc. Ind.* **2003**, *16*, 457–478. [CrossRef]
25. Egolfopoulos, F.N.; Hansen, N.; Ju, Y.; Kohse-Höinghaus, K.; Law, C.K.; Qi, F. Advances and challenges in laminar flame experiments and implications for combustion chemistry. *Prog. Energy Combust. Sci.* **2014**, *43*, 36–67. [CrossRef]
26. Lipatnikov, A.N.; Shy, S.S.; Li, W. Experimental assessment of various methods of determination of laminar flame speed in experiments with expanding spherical flames with positive Markstein lengths. *Combust. Flame* **2015**, *16*, 22840–22854. [CrossRef]
27. Hassan, M.I.; Aung, K.T.; Faeth, G.M. Measured and predicted properties of laminar premixed methane/air flames at various pressures. *Combust. Flame* **1998**, *11*, 539–550. [CrossRef]
28. Gu, X.J.; Haq, M.Z.; Lawes, M.; Woolley, R. Laminar burning velocity and Markstein lengths of methane–air mixtures. *Combust. Flame* **2000**, *121*, 41–58. [CrossRef]
29. Duva, C.B.; Wang, C.Y.; Chance, L.E.; Toulson, E. Correlations for the laminar burning velocity and burned gas Markstein length of methane-air mixtures diluted with flue gases at high temperatures and pressures. *Fuel* **2020**, *281*, 118721. [CrossRef]
30. Varghese, R.J.; Kolekar, H.; Kishore, R.; Kumar, S. Measurement of laminar burning velocities of methane-air mixtures simultaneously at elevated pressures and elevated temperatures. *Fuel* **2019**, *25*, 116120. [CrossRef]
31. Salzano, E.; Pioa, G.; Ricca, A.; Palma, V. The effect of a hydrogen addition to the premixed flame structure of light alkanes. *Fuel* **2018**, *234*, 1064–1070. [CrossRef]
32. Pagliaro, J.L.; Linteris, G.T.; Sunderland, P.B.; Baker, P.T. Combustion inhibition and enhancement of premixed methane–air flames by halon replacements. *Combust. Flame* **2015**, *162*, 41–49. [CrossRef]
33. Chan, Y.L.; Zhu, M.M.; Zhang, Z.Z.; Liu, P.F.; Zhang, D.K. The Effect of CO2 dilution on the laminar burning velocity of premixed methane/air flames. *Energy Procedia* **2015**, *75*, 3048–3053. [CrossRef]
34. Park, O.; Veloo, P.S.; Liu, N.; Egolfopoulos, F.N. Combustion characteristics of alternative gaseous fuels. *Proc. Combust. Inst.* **2011**, *33*, 887–894. [CrossRef]
35. Akram, M.; Saxena, P.; Kumar, S. Laminar burning velocity of methane–air mixtures at elevated temperatures. *Energy Fuels* **2013**, *27*, 3460–3466. [CrossRef]
36. Konnov, A.; Akram, M.; Kishore, V.R.; Kim, N.; Pratha, C.; Kumar, S. A comprehensive review of measurements and data analysis of laminar burning velocities for various fuel+airmixtures. *Prog. Energy Combust. Sci.* **2018**, *68*, 197–267. [CrossRef]
37. Razus, D.; Oancea, D.; Movileanu, C. Burning velocity evaluation from pressure evolution during the early stage of closed-vessel explosions. *J. Loss Prevent. Proc. Ind.* **2006**, *19*, 334–342. [CrossRef]
38. Razus, D.; Oancea, D.; Brinzea, V.; Mitu, M.; Movileanu, C. Experimental and computed burning velocities of propane–air mixtures. *Energy Convers. Manag.* **2010**, *51*, 2979–2984. [CrossRef]
39. Razus, D.; Brinzea, V.; Mitu, M.; Oancea, D. Burning Velocity of Liquefied Petroleum Gas (LPG)−air mixtures in the presence of exhaust gas. *Energy Fuel* **2010**, *24*, 1487–1494. [CrossRef]

40. Movileanu, C.; Razus, D.; Oancea, D. Additive Effects on the Burning Velocity of Ethylene–Air Mixtures. *Energy Fuel* **2011**, *25*, 2444–2451. [CrossRef]
41. Razus, D.; Brinzea, V.; Mitu, M.; Movileanu, C.; Oancea, D. Burning velocity of propane–air mixtures from pressure–time records during explosions in a closed spherical vessel. *Energy Fuels* **2012**, *26*, 901–909. [CrossRef]
42. Mitu, M.; Razus, D.; Giurcan, V.; Oancea, D. Normal burning velocity and propagation speed of ethane–air: Pressure and temperature dependence. *Fuel* **2015**, *147*, 27–34. [CrossRef]
43. Brinzea, V.; Mitu, M.; Movileanu, C.; Musuc, A.; Razus, D. Expansion coefficients and normal burning velocities of propane-air mixtures by the closed vessel technique. *Buchar. Univ. Chem. Fac. Ann.* **2010**, *19*, 31–37.
44. Bradley, D.; Mitcheson, A. Mathematical solutions for explosions in spherical vessels. *Combust. Flame* **1976**, *26*, 201–217. [CrossRef]
45. Metghalchi, M.; Keck, J. Laminar burning velocity of propane-air mixtures at high temperature and pressure. *Combust. Flame* **1980**, *38*, 143–154. [CrossRef]
46. Huzayyin, A.S.; Moneib, H.A.; Shehatta, M.S.; Attia, A.M.A. Laminar burning velocity and explosion index of LPG–air and propane–air mixtures. *Fuel* **2008**, *87*, 39–57. [CrossRef]
47. Andrews, G.; Bradley, D. The burning velocity of methane-air mixtures. *Combust. Flame* **1972**, *19*, 275–288. [CrossRef]
48. Potter, A.E., Jr.; Berlad, A.L. The effect of fuel type and pressure on flame quenching. *Symp. Int. Combust.* **1957**, *6*, 27–36. [CrossRef]
49. Lewis, B.; von Elbe, G. *Combustion Flames and Explosion of Gases*; Academic Press: New York, NY, USA, 1987; Chapter 5.
50. Moorhouse, J.; William, A.; Maddison, T.E. An investigation of the minimum ignition energies of some C1 to C7 hydrocarbons. *Combust. Flame* **1974**, *23*, 203–213. [CrossRef]
51. Zhang, B.; Bai, C.; Xiu, G.; Liu, Q.; Gong, G. Explosion and flame characteristics of methane/air mixtures in a large-scale vessel. *Process. Saf. Progr.* **2014**, *33*, 362–368. [CrossRef]
52. Tang, C.; Zhang, S.; Si, Z.; Huang, Z.; Zhang, K.; Jin, Z. High methane natural gas/air explosion characteristics in confined vessel. *J. Hazard. Mater.* **2014**, *278*, 520–528. [CrossRef]